Hindawi
Shock and Vibration
Volume 2019, Article ID 3904595, 9 pages
https://doi.org/10.1155/2019/3904595

Research Article

Vibration Analysis of a Single-Cylinder Reciprocating Compressor considering the Coupling Effects of Torsional Vibration

Siyuan Liu, Wanyou Li, Zhijun Shuai, and Meilong Chen

College of Power and Energy Engineering, Harbin Engineering University, Harbin 150001, China

Correspondence should be addressed to Zhijun Shuai; shuaizhijun98@163.com

Received 21 January 2019; Accepted 7 March 2019; Published 1 April 2019

Academic Editor: Sumeet S. Aphale

A piston slap is one of the main vibration sources of the reciprocating machinery. Much work has been done in this field, most of which was based on a constant rotating speed. However, in practice, the speed of a crankshaft may always fluctuate due to the uneven load or excitation. The inertia forces of moving components are much different at the fluctuating rotating speed comparing with that at a constant speed. In this paper, the piston slap and the induced vibration are analyzed based on the instantaneous angular speed measured on a single-cylinder reciprocating compressor. Firstly, the dynamics of a crank-connecting rod mechanism is analyzed based on the measured instantaneous angular speed which contains the torsional vibration of the air compressor. The time histories of piston slap impact forces considering and without considering torsional vibration are compared. Then, in order to correlate the piston slap impact with the slap-induced vibration, the corresponding transfer functions between the middle stroke of the outer surface of the cylinder liner and the excitation points are measured. And the excitation force on the main bearing is also taken into account to bring the simulation closer to the experimental results. The effects of a torsional vibration on the vibration of the cylinder liner are analyzed, and the simulation results show that the torsional vibration is a factor that must be taken into account in the vibration analysis of the single-cylinder reciprocating compressor.

1. Introduction

A piston slap, the impact caused by the sidewise motions of pistons across the cylinder clearance spaces, has long been recognized to be a major source of noise and vibration in reciprocating machinery. And this phenomenon has been investigated from both analytical and experimental points of view for over fifty years. Ungar and Ross attempt to estimate the vibration and noise power levels induced by the piston slap for the first time [1]. The piston slap at TDC has been simulated by Haddad and Fortescue in an analogue computer [2], and the effects of oil film on piston slap excitation were considered in his following studies [3]. Ryan [4] and Rèpaci [5] analyzed the effect of the change in engine operating and geometric parameters on piston slap impact force through experiments and simulations. Simultaneous noise reduction in the conditions of both idling and high speed was achieved by Nakashima et al. [6].

There have been many models developed to estimate the impact forces and the side-thrust force. A lumped parameter model of the piston and liner was developed to describe the dynamics of the piston slap, and the model parameters are obtained from mobility measurement. This model was used to estimate the overall vibration level at the engine block surface [7]. There is another lumped parameter model with eight degrees of freedom which is developed using the dynamic characteristics of the piston, connecting rod, cylinder wall, and engine block. In [8], the time history of the piston slap force is determined, and the

spectra of the force are compared for different operational regimes of the engine. A finite element method (FEM) has also been applied in order to analyze the impact forces [9]. The models, as well as FEM, are not satisfactory to estimate the impact forces. The relative motion between piston and cylinder liner is actually a lubrication process. So many mathematical models were based on the Reynolds equation [10–12]. However, almost all models are difficult to analyze the exact frequency of piston-induced vibration and can only be used as an estimate of overall vibrational energy.

In addition, reciprocating machinery always has some degrees of torsional vibration (TV) during operation due to their reciprocating nature. But relatively few studies appear to have been done on the relations between torsional vibrations and linear or block vibration. In general, the effect of torsional vibration has been ignored in the recent piston slap studies. Whilst the crankshaft of an engine rotates with TV, the inertial forces of the piston, connecting rod, and crankshaft fluctuate, and the dynamics of the piston is affected both on reciprocating and secondary orientations. Many researchers have pointed it out that the combustion noise and the piston slap noise are found to be overlapped in the time domain and frequency domain [13–15]. However, the exact frequency range of the vibration caused by the piston slap is hard to determine with the interference of combustion noise. In order to solve this problem, a single-cylinder air compressor where the combustion noise is absent is selected as the research object in this paper.

At the beginning of this paper, the instantaneous angular speed is measured on a single-cylinder reciprocating compressor whose medium-low-frequency vibration is mainly concentrated in 100–350 Hz. Based on the instantaneous angular speed, the dynamics of the crank-connecting rod mechanism is analyzed. The time histories of piston slap impact forces considering and without considering torsional vibration are compared. Then, in order to correlate the piston slap impact with the slap-induced vibration, the corresponding transfer functions between the middle stroke of the outer surface of the cylinder liner and the excitation points are measured. And the excitation force on the main bearing is also taken into account to bring the simulation closer to the experimental results. The effects of the torsional vibration on the vibration of the cylinder liner are analyzed, and the simulation results show that the torsional vibration contributes greatly to the vibration of the cylinder liner vibration.

2. Experimental Configuration

The test bench is a motor-driven single-cylinder air compressor with a bearing in the middle of a rotating shaft and two inertia disks on each side of the bearing. Teeth are machined on the edge of the inertia disks for measuring the instantaneous angular speed. And an elastic coupling made of polyurethane material is mounted inside the bigger inertia disk. The arrangement of the compressor is shown in Figure 1.

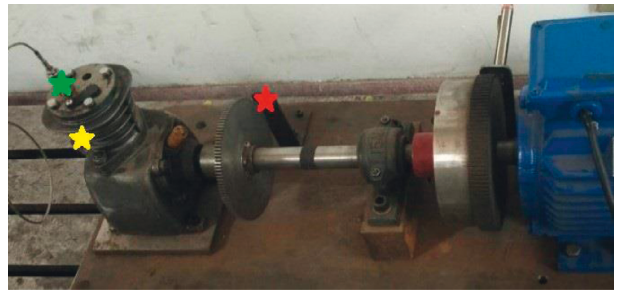

Figure 1: Arrangement of the compressor.

To measure the acceleration, pressure, and instantaneous angular speed signal of such a compressor, a *B&K* 4526 single-direction accelerometer, a *Kisler* 6125A pressure transducer, and a magnetoelectric sensor are used. The signal is collected and processed in a *B&K PULSE* 3560B. In Figure 1, the gage map for the accelerometer (yellow star), the pressure sensor (green star), and the magnetoelectric sensor (red star) which is used to measure the instantaneous angular speed of the compressor are illustrated.

3. Experimental Results

The rotating speed is set to 400 rpm, and the instantaneous angular speed within one cycle is shown in Figure 2. Figure 2(a) demonstrates the raw signal of the electromagnetic transducer, and it can be used to calculate the instantaneous angular speed. As it is shown in Figure 2(b), the fluctuation range is about 5%.

The variation of the pressure inside the cylinder during an intake and exhaust cycle is shown in Figure 3. The piston is at the top dead center in the initial position. And Figure 4 shows the acceleration response of the cylinder liner outer wall. It can be seen that the medium-low-frequency vibration of the cylinder liner is mainly concentrated in 100–350 Hz. In this paper, the influence of torsional vibration on the piston slap-induced vibration in this frequency band will be analyzed.

Based on the above measurements, the dynamics of the crank-connecting rod mechanism is analyzed in the following part.

4. Primary Motions and Inertia Forces of Machine Components considering TV

The forces acting within the compressor may most readily be studied with the aid of a diagram shown in Figure 5. The left part of this figure describes the geometry of a typical crank-connecting rod mechanism, defines the sign conventions used in this paper, and serves as a basis for the determination of the motions and inertia forces of the moving components. These forces and the pertinent interaction forces are demonstrated in the "free body" diagrams of the crank, connecting rod, and piston which appear in the right portion of the figure.

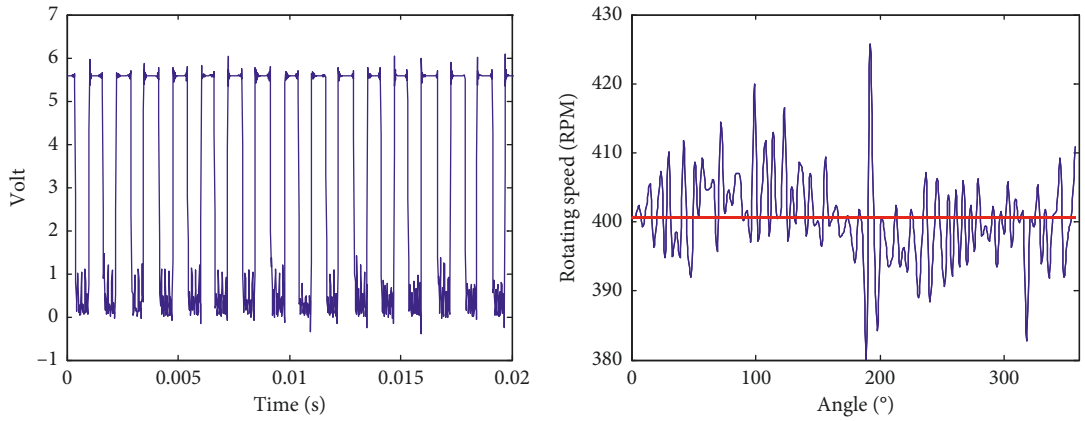

Figure 2: (a) Raw signal for speed measurement. (b) The measured instantaneous angular speed.

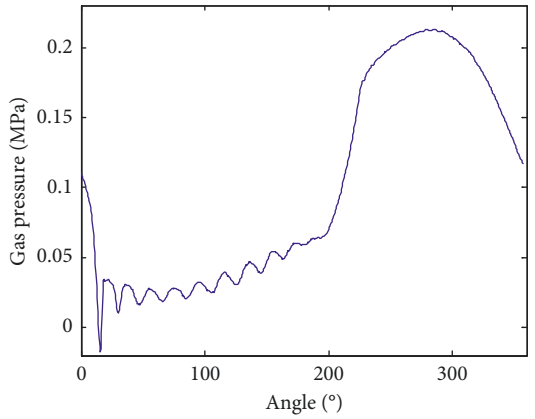

Figure 3: Variation of in-cylinder pressure.

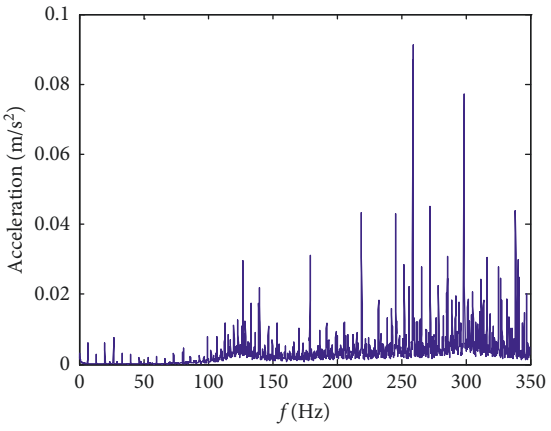

Figure 4: Vibration of the cylinder liner.

α stands for the crank angle, and if the rotating speed is constant without any fluctuation, $\dot{\alpha} = \text{const}$, and $\ddot{\alpha} = 0$. While considering the torsional vibration, the angular velocity is not a constant any more and angular acceleration $\ddot{\alpha} \neq 0$.

The piston motion is expressed as the crankshaft angle function as follows:

$$x_p = R(1-\cos\alpha) + L\left(1-\sqrt{1-\lambda^2\sin^2\alpha}\right),$$

$$v_p = \dot{x}_p = \left(R\sin\alpha + \frac{L\lambda^2\sin\alpha\cos\alpha}{\sqrt{1-\lambda^2\sin^2\alpha}}\right)\dot{\alpha},$$

$$a_p = \ddot{x}_p = \left(R\sin\alpha + \frac{L\lambda^2\sin 2\alpha}{2\sqrt{1-\lambda^2\sin^2\alpha}}\right)\ddot{\alpha} + \left(R\cos\alpha + L\lambda^2\left(\frac{\cos 2\alpha}{\sqrt{1-\lambda^2\sin^2\alpha}} + \frac{\lambda^2\sin^2 2\alpha}{4\left(1-\lambda^2\sin^2\alpha\right)^{3/2}}\right)\right)\dot{\alpha}^2. \quad (1)$$

Take the measured instantaneous angular velocity into the formula, and the angular acceleration can be obtained by calculating the first derivative of the velocity to time. The difference in the piston motion considering and without considering TV is shown in Figure 6.

4.1. Piston Side-Thrust Force and Extra Piston Slaps due to the Torsional Vibration. The piston side-thrust force is derived from the forces and moment of the crankshaft, connecting rod, and piston. It can be deduced from the equations of the system as shown below:

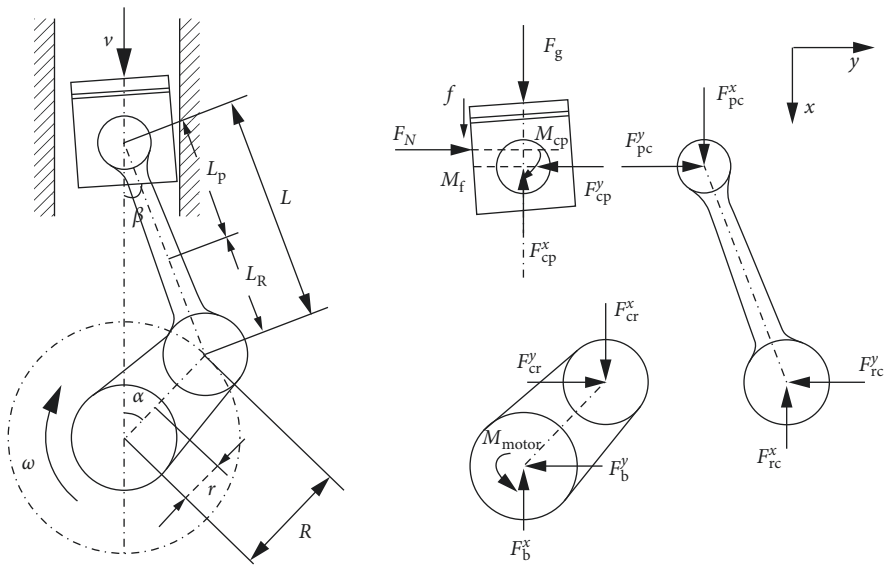

Figure 5: Piston and connecting rod geometry and forces.

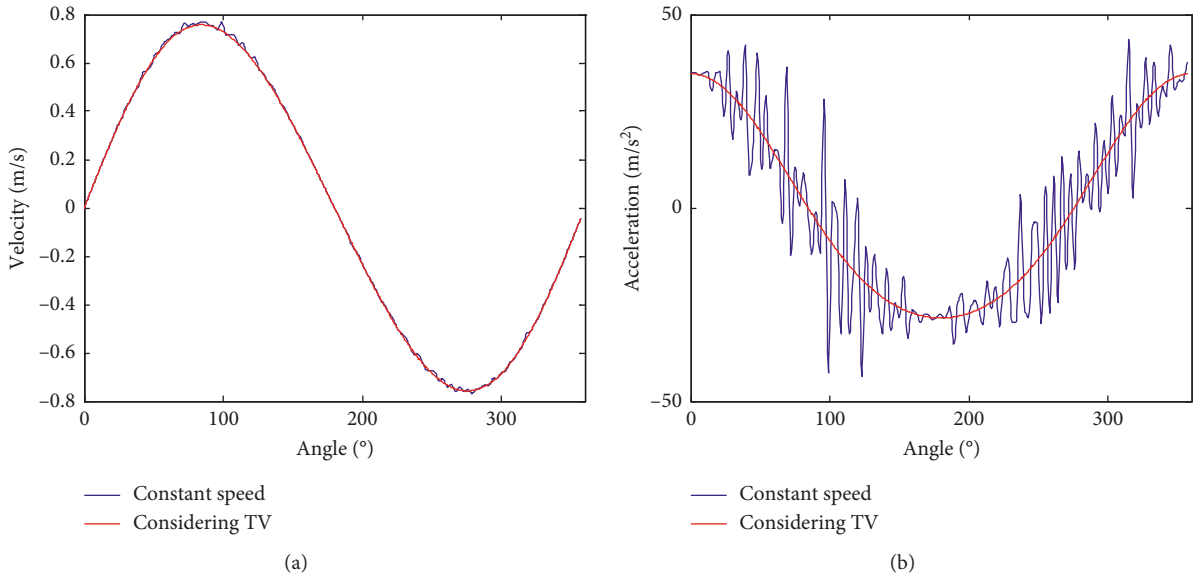

Figure 6: Piston speed (a) and acceleration (b) with and without TV.

$$\begin{bmatrix} m_p & & & & & & & & \\ & m_p & & & & & & & \\ & & J_p & & & & & & \\ & & & m_c & & & & & \\ & & & & m_c & & & & \\ & & & & & J_c & & & \\ & & & & & & m_r & & \\ & & & & & & & m_r & \\ & & & & & & & & J_r \end{bmatrix} \begin{Bmatrix} a_p^x \\ a_p^y \\ \ddot{\alpha}_p \\ a_c^x \\ a_c^y \\ \ddot{\alpha}_c \\ a_r^x \\ a_r^y \\ \ddot{\alpha} \end{Bmatrix} = \begin{Bmatrix} F_N + F_{cp}^x \\ F_g + F_{cp}^y + f \\ M_f + M_{cp} \\ F_{pc}^x + F_{rc}^x \\ F_{pc}^y + F_{rc}^y \\ M_{pc} + M_{rc} \\ F_{cr}^x + F_b^x \\ F_{cr}^y + F_b^y \\ M_{cr} + M_{motor} \end{Bmatrix}. \quad (2)$$

The clearance between the piston skirt and the cylinder liner is only 10 μm, which makes the inertial force of the piston in the y direction neglectable. The main driving force of the piston slap-induced vibration is the piston side-thrust force which acts on the piston skirt imparted by the piston connecting rod. From the equations, one may solve for the side-thrust force F_N which takes into account the effect of the variation of the system inertia with respect to the rotation angle of the crankshaft:

$$\psi_s = \frac{F_N}{m_p R\omega^2\lambda} = \psi_g - \left(\psi_p + \psi_c\right), \tag{3}$$

where

$$\psi_g = \frac{F_g \tan\beta}{m_p R\omega^2\lambda},$$

$$\psi_p = \frac{F_p^x \tan\beta}{m_p R\omega^2\lambda}, \tag{4}$$

$$\psi_c = \frac{\left(F_c^y + F_c^x \tan\beta\right)L_R \cos\beta + J_c\ddot{\beta}}{L(\cos\beta)m_p R\omega^2\lambda}.$$

To analyze the effect of the torsional vibration on each part of the side-thrust force, a dimensionless side-thrust force parameter ψ_s is divided into three parts based on the method reported in [1]. ψ_g, ψ_p, and ψ_c represent the contributions to the value of this parameter made by the gas force, the piston inertia, and the connecting rod inertia, respectively.

The term $m_p R\omega^2\lambda$, which has been used as a normalization factor in equation (3), may be treated as representing the centrifugal force that the piston would exert if it were a point mass attached to the rotating crankshaft at the crank radius.

Secondary motion of the piston across the cylinder clearance could be recognized to be initiated if the side-thrust force F_N acting on the piston changes the direction. Therefore, when the right-hand side of equation (3) changes its algebraic sign or equals zero, the crank angle α is the initiated position of the piston slap. It can easily be seen that the initiated positions are for $\psi_g = (\psi_p + \psi_c)$. Figure 7 shows the condition of the piston slap when the rotating speed is constant. The left portion of this figure demonstrates the contribution of the piston and connecting rod inertia to the piston slap. And the right portion shows the initiated position of secondary motion of the piston. The curve of ψ_g intersects the curve of $(\psi_p + \psi_c)$, not only at the top dead center ($\alpha = 0^\circ$) and bottom dead center ($\alpha = 180^\circ$), but also at a mid-stroke" position during the intake stroke for the selected compressor in this paper.

When TV is considered, the conditions will vary enormously as is shown in Figure 8. The inertial force of the piston slap and connecting rod fluctuate greatly because of the nonzero rotational acceleration of the crankshaft. There are more intersections around the three positions than those at the constant speed. The number of times F_N changes sign increased from 3 to 22. Therefore, the torsional vibration will definitely affect the piston slap and its induced vibration. Figure 9 compares the side-thrust force F_N with and without TV.

4.2. Main Bearing Reacting Force. The main bearing reacting force is numerically equal to the normal force exerted by the connecting rod on the crank, which can be obtained by solving equation (2):

$$F_{\text{bearing}}^x = \left(F_{cr}^y \sin\alpha - F_{cr}^x \cos\alpha - m_r\omega^2 r\right)\cos\alpha,$$
$$F_{\text{bearing}}^y = -\left(F_{cr}^y \sin\alpha - F_{cr}^x \cos\alpha - m_r\omega^2 r\right)\sin\alpha, \tag{5}$$

where m_r and r represent the equivalent rotational mass and radius of the crank, respectively. The results of the main bearing reacting force with and without torsional vibration are shown in Figure 10.

5. The Effect of TV on the Vibration of the Cylinder Liner

In order to calculate the vibration of the cylinder liner, three transfer functions are measured. One of them is measured between the middle stroke of the inner and outer walls of the cylinder liner. The other two are measured between the outer wall and the main bearing excitation point in horizontal and vertical directions. These transfer functions are used to calculate the vibration of the cylinder liner. In the measurement of these transfer functions, the cylinder head is removed and one accelerometer is fixed on the outside of the cylinder wall at the middle stroke, and the transfer function between inside and outside the cylinder liner is obtained by hitting the inner wall of the cylinder liner at the middle stroke with an impact hammer. The other two transfer functions are measured by hitting the horizontal and vertical directions of the shaft section at the joint of the main bearing. In [7], the transfer functions are used to predict the vibratory response in the frequency range below about 500 Hz. And it will also be used to calculate the vibration of the cylinder liner in the frequency bands of interest in this paper, which is 100–350 Hz, the most intense frequency band of the given compressor. The measured transfer functions between excitation forces and the vibration acceleration are expressed in Figure 11. In this figure, H1 represents the transfer function of the inner wall of the cylinder liner and the response point. H2 represents the transfer function of the horizontal direction of the main bearing position and the response point, and H3 represents the transfer function of the vertical direction of the main bearing position and the response point.

The vibration of the cylinder liner can be obtained by adding the calculated force with and without TV into the measured transfer functions. This system can be defined by the basic transform relation [16]:

$$Y(f) = H_1(f)X_1(f) + H_2(f)X_2(f) + H_3(f)X_3(f) + N(f). \tag{6}$$

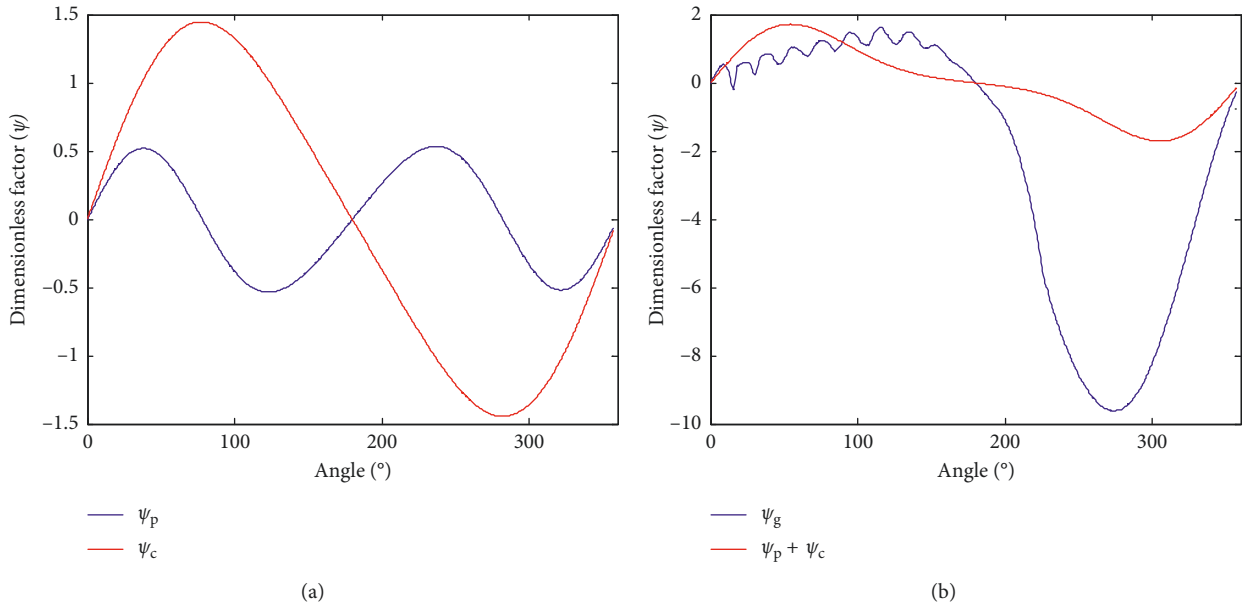

Figure 7: Inertia and gas force contributions to the piston slap without TV.

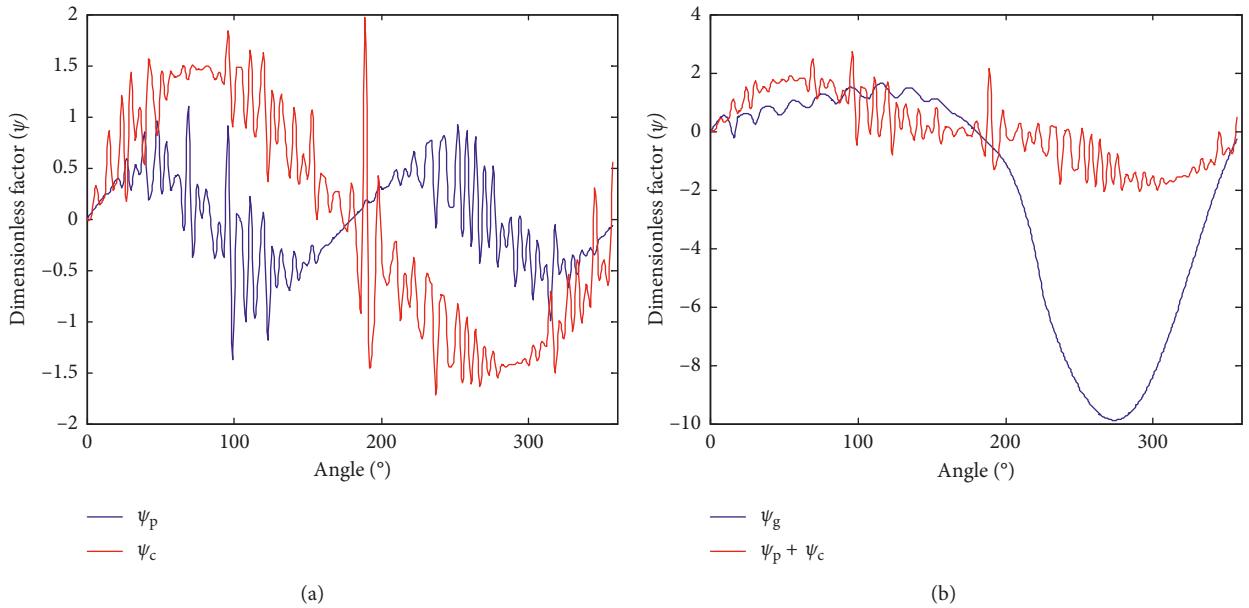

Figure 8: Inertia and gas force contributions to the piston slap with TV.

For arbitrary $n(t)$, which may be correlated with $x_1(t)$ and/or $x_2(t)$ and $x_3(t)$, the one-sided autospectral density function of $y(t)$ for a very long but finite record length T is given by

$$\begin{aligned} G_{yy} &= \frac{2}{T} E(Y^* Y), \\ &= \frac{2}{T} E\left[\{H_1^* X_1^* + H_2^* X_2^* + H_3^* X_3^* + N^*\}\right. \\ &\quad \left. \cdot \{H_1 X_1 + H_2 X_2 + H_3 X_3 + N\}\right]. \end{aligned} \tag{7}$$

When $n(t)$ is uncorrelated with $x_i(t)$, equation (6) becomes

$$G_{yy} = \begin{Bmatrix} H_1^* \\ H_2^* \\ H_3^* \end{Bmatrix}^T \begin{bmatrix} G_{11} & G_{12} & G_{13} \\ G_{21} & G_{22} & G_{23} \\ G_{31} & G_{32} & G_{33} \end{bmatrix} \begin{Bmatrix} H_1 \\ H_2 \\ H_3 \end{Bmatrix} + G_{nn}. \tag{8}$$

Figure 12 compares the estimated vibration and measured vibration. The main frequency interval of vibration is 6.67 Hz, which is the fundamental frequency of the shaft. As shown in the figure, without considering the torsional

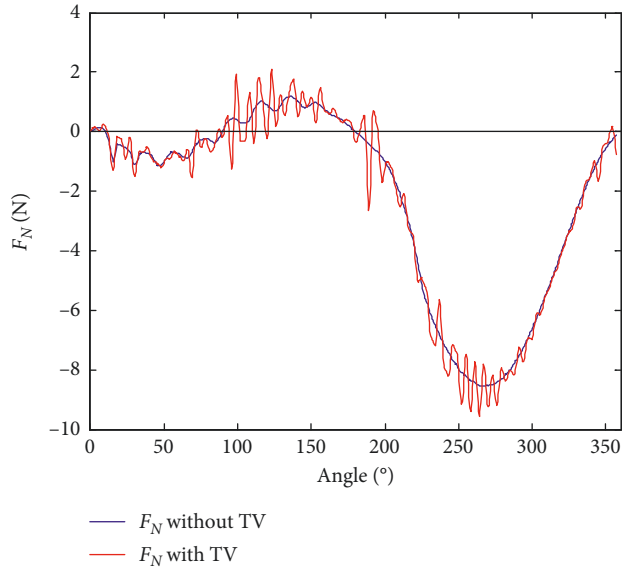

Figure 9: Side-thrust force F_N with and without TV.

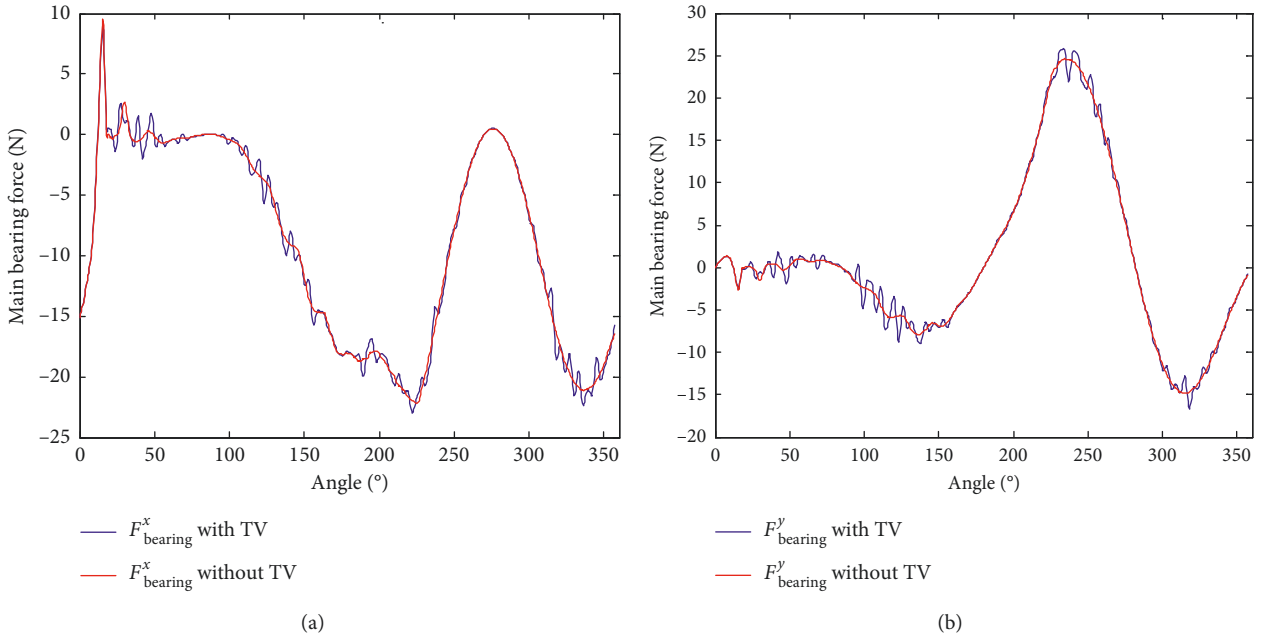

Figure 10: Main bearing reacting force with and without TV.

vibration, the shaft rotates at a steady and constant speed, and the piston slap force and the main bearing force only contribute to the vibration in the frequency range of 100–150 Hz. There is almost no contribution between 200 and 350 Hz, where the vibration is more intense. However, if torsional vibration is taken into account, it can be seen that these forces not only contributes between 100 and 150 Hz but also within 150–350 Hz.

In order to make the contrast clearer, the overall acceleration level is calculated within each 50 Hz band as shown in Table 1.

Figure 13 shows the corresponding bar graph of the comparison between estimated and measured vibration acceleration level at the cylinder liner outer wall in the selected motoring condition. As shown in Figure 13, if the TV is not considered, the smallest error is 6.7 dB which is between 100 and 150 Hz and all the rest errors are larger than 20 dB. This is unacceptable. In contrast, considering TV's response is far superior to not considering TV and closer to the measured response. In 4 of the 5 frequency bands, the calculation error is within 2.5 dB, and only 250–300 Hz has a larger error. The reason is that the two largest line spectra, 260 Hz and 300 Hz, are not caused by the forces considered and may be caused by other excitation, such as the slap of the intake and exhaust valves; the relevant work will be verified in subsequent studies.

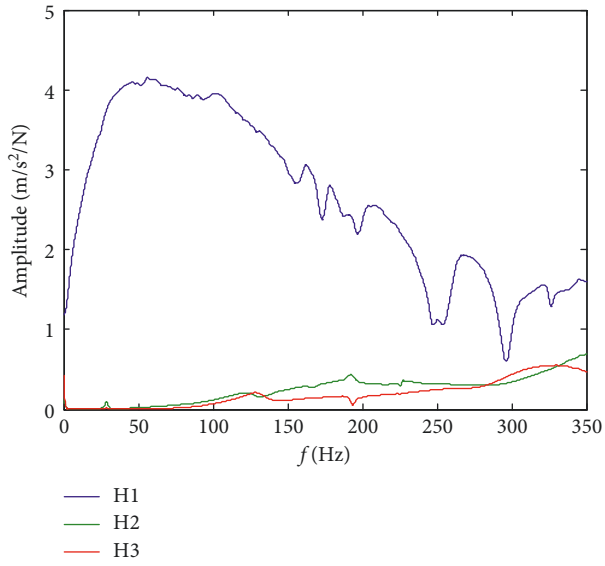

Figure 11: Measured transfer functions of the cylinder.

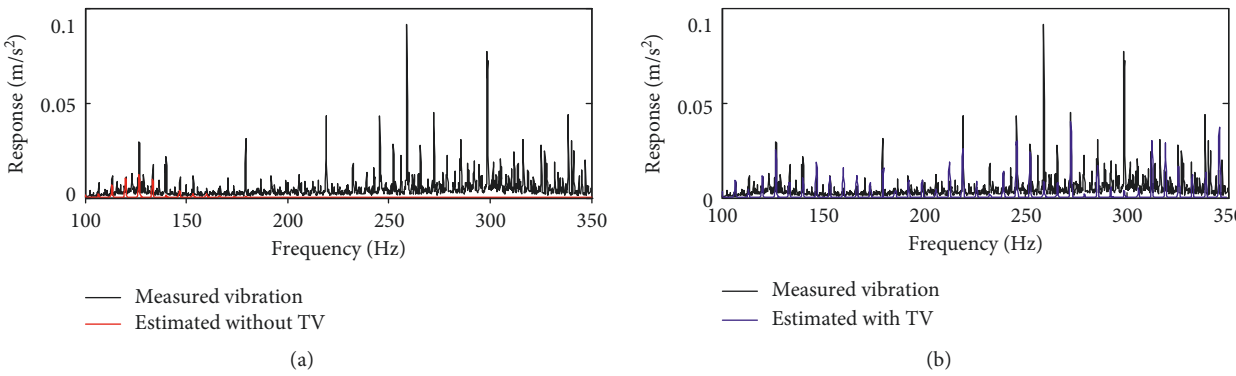

Figure 12: Comparison between estimated and measured vibration.

Table 1: Overall acceleration level between estimated and measured vibration.

	100–150 Hz	150–200 Hz	200–250 Hz	250–300 Hz	300–350 Hz
Estimation without TV	92.8	76.4	59.4	56.7	56.4
Estimation with TV	97.7	96.2	100.2	100.7	102.1
Measured vibration	99.5	97.5	102.4	108.5	104.6

It can be seen that the torsional vibration is a factor that must be taken into account when calculating the vibration of the cylinder liner, as the reciprocating air compressors or internal-combustion engines are often accompanied by violent speed fluctuations due to uneven load or excitation.

6. Conclusions

In this paper, a torsional vibration coupled dynamics analysis of a crank-connecting rod mechanism has been presented. The result shows that when the torsional vibration is considered, the corresponding fluctuations in the inertia forces of the piston and connecting rod have a great influence on piston slap force.

Then the vibration of the cylinder liner is estimated approximately based on the measured transfer functions. The estimated vibrations demonstrate that the piston slap force and the main bearing force contribute not only to the vibration between 100 and 150 Hz but also to the vibration in the higher frequency bands, and this can be observed only when the torsional vibration is considered. Finally, the prediction of overall vibration level shows the necessity of torsional vibration in the vibration analysis of the single-cylinder reciprocating compressor. This result is also applicable to vibration prediction of other reciprocating mechanical equipment. What needs special attention is that the frequency bands being analyzed can be different according to the characteristics of the given engine or compressor, and

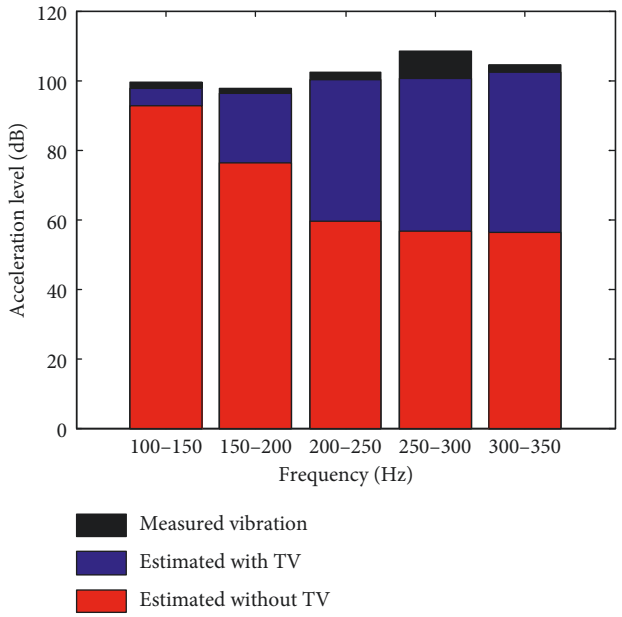

Figure 13: The overall acceleration level between estimated and measured vibration.

100–350 Hz was just for the specific compressor in this paper.

Data Availability

The data that support the findings of this study are available from the corresponding author [Siyuan L, Zhijun S, Wanyou L, Meilong Chen], upon reasonable request.

Conflicts of Interest

The authors declare that they have no conflicts of interest.

References

[1] E. E. Ungar and D. Ross, "Vibrations and noise due to piston-slap in reciprocating machinery," *Journal of Sound and Vibration*, vol. 2, no. 2, pp. 132–146, 1965.

[2] S. D. Haddad and P. W. Fortescue, "Simulating piston slap by an analogue computer," *Journal of Sound and Vibration*, vol. 52, no. 1, pp. 79–93, 1977.

[3] S. D. Haddad and K.-T. Tjan, "An analytical study of offset piston and crankshaft designs and the effect of oil film on piston slap excitation in a diesel engine," *Mechanism and Machine Theory*, vol. 30, no. 2, pp. 271–284, 1995.

[4] J. P. Ryan, *Impact Analysis of Piston Slap in a Spark Ignition Engine*, Massachusetts Institute of Technology, Cambridge, MA, USA, 1993.

[5] A. Rèpaci, "Non linear modelling of the piston slap phenomenon in an alternative internal combustion engine," *Mathematical Modelling*, vol. 8, pp. 366-367, 1987.

[6] K. Nakashima, Y. Yajima, and K. Suzuki, "Approach to minimization of piston slap force for noise reduction a investigation of piston slap force by numerical simulation," *JSAE Review*, vol. 20, no. 2, pp. 211–216, 1999.

[7] S.-H. Cho, S.-T. Ahn, and Y.-H. Kim, "A simple model to estimate the impact force induced by piston slap," *Journal of Sound and Vibration*, vol. 255, no. 2, pp. 229–242, 2002.

[8] S. N. Y. Gerges, J. C. De Luca, and N. Lalor, "The influence of cylinder lubrication on piston slap," *Journal of Sound and Vibration*, vol. 257, no. 3, pp. 527–557, 2002.

[9] K. Ohta, Y. Irie, K. Yamamoto et al., "Piston slap induced noise and vibration of internal combustion engines (1st report, theoretical analysis and simulation)," in *SAE Technical Paper Series*, pp. 133–138, SAE International, Warrendale, PA, USA, 1987.

[10] D. F. Li, S. M. Rohde, and H. A. Ezzat, "An automotive piston lubrication model," *A S L E Transactions*, vol. 26, no. 2, pp. 151–160, 1983.

[11] D. Zhu, H. S. Cheng, T. Arai, and K. Hamai, "A numerical analysis for piston skirts in mixed lubrication-part I: basic modeling," *Journal of Tribology*, vol. 114, no. 3, pp. 553–562, 1992.

[12] L. Yanjun, L. Sha, W. Peng et al., "The analysis of secondary motion and lubrication performance of piston considering the piston skirt profile," *Shock and Vibration*, vol. 2018, Article ID 3240469, 27 pages, 2018.

[13] J. Yao, Y. Xiang, S. Qian, S. Wang, and S. Wu, "Noise source identification of diesel engine based on variational mode decomposition and robust independent component analysis," *Applied Acoustics*, vol. 116, pp. 184–194, 2017.

[14] M. E. Badaoui, J. Danière, F. Guillet, and C. Servière, "Separation of combustion noise and piston-slap in diesel engine-part I: separation of combustion noise and piston-slap in diesel engine by cyclic Wiener filtering," *Mechanical Systems and Signal Processing*, vol. 19, no. 6, pp. 1209–1217, 2005.

[15] C. Servière, J.-L. Lacoume, and M. El Badaoui, "Separation of combustion noise and piston-slap in diesel engine-part II: separation of combustion noise and piston-slap using blind source separation methods," *Mechanical Systems and Signal Processing*, vol. 19, no. 6, pp. 1218–1229, 2005.

[16] J. S. Bendat and A. G. Piersol, *Random Data: Analysis and Measurement Procedures Random Data Analysis and Measurement Procedures*, John Wiley & Sons, Hoboken, Nj, USA, 1971.